ELSEVIER

Polymer 41 (2000) 5653–5660

polymer

Microstructure-tensile properties relationships of polyurethane/poly(urethane-modified bismaleimide–bismaleimide) interpenetrating polymer networks

Yuanli Cai[a,b,*], Pengsheng Liu[a], Xianbo Hu[b], Dujin Wang[b], Duanfu Xu[b]

[a]*College of Chemistry and Chemical Engineering, Xiangtan University, Hunan, 411105, People's Republic of China*
[b]*Group 507, Institute of Chemistry, The Chinese Academy of Sciences, Beijing, 100080, People's Republic of China*

Received 30 June 1999; received in revised form 30 August 1999; accepted 18 October 1999

Abstract

A series of polyurethane/poly(urethane-modified bismaleimide–bismaleimide) interpenetrating polymer networks (PU/P(UBMI–BMI) IPNs) including semi-IPNs and full-IPNs were synthesized. The microstructures were examined by TEM. The effects of the ratios of UBMI/BMI, molecular weight of PBAG in UBMI and P(UBMI–BMI)/PU on tensile strength and elongation at break were investigated. The fractograghs were examined by SEM. The results indicate that interpenetration occurs at the hard segment domains of PU, which leads to enhancement of phase separation of PU and the dispersing tendency of dispersed phase of IPNs. Mobility and interlocking of the chains are important factors affecting the formation of this particular structure in the dispersed phase, they must be considered together to satisfy the demand for comprehensive positive synergistic effect on tensile properties. This particular structure can delay crack resource formation and retard crack propagation, leading to improvement of strength and toughness of PU/P(UBMI–BMI) IPNs.

Keywords: PU/P(UBMI–BMI) IPNs; Interpenetrating structure of the dispersed phase; Tensile properties

1. Introduction

Owing to synergistic deformation and thermal response, by means of interpenetration, and enhanced mutual entanglement between two polymer networks, interpenetrating polymer networks (IPNs) elastomers usually have mechanical and thermal properties in excess of those exhibited by blends having the same constituents prepared in other blending ways [1–6].

In a previous paper [6], we have synthesized polyurethane/poly(urethane-modified bismaleimide–bismaleimide) interpenetrating polymer networks (PU/P(UBMI–BMI) IPNs), studied the chemical structure and compatibility of the two polymer networks and determined the domain dimensions of the dispersed phases. The results indicate that interpenetration of PU and P(UBMI–BMI) obviously affects the hydrogen bonding of N–H. The ratio of UBMI and BMI in P(UBMI–BMI) is one of the key factors influencing hydrogen bonding. Hydrogen bonding is enhanced dramatically when UBMI/BMI is in the range of 40/60 to 60/40. Interpenetration of the two networks retards the destruction of hydrogen bonds and the pyrolysis of urethane, that is, PU/P(UBMI–BMI) IPNs show better thermal stability than PU.

Based on the traditional classification of IPNs, IPNs in which both polymer components are covalently cross-linked are defined as full-IPNs, while, only one polymer component is covalently cross-linked, are defined as semi-IPNs. In this work, we have synthesized a series of PU/P(UBMI–BMI) IPNs (including full-IPNs whose PU is cross-linked by trimethylol propane, and semi-IPNs whose PU is not cross-linked), investigated the IPNs' occurrence area and their nature. The tensile properties were tested and the morphologies of the fracture surfaces were also examined and discussed.

2. Experimental

2.1. Preparation of PU/P(UBMI–BMI) IPNs

The method for preparation of full-IPNs is the same as that in Ref. [6]. Semi-IPNs were synthesized in two steps.

* Corresponding author. Address: Group 507, Institute of Chemistry, The Chinese Academy of Sciences, Beijing 10080, People's Republic of China. Tel.: +86-10-6256-2961; fax: +86-10-6255 9373.
E-mail address: xudf@infoc3.icas.ac.cn (Y. Cai).

0032-3861/00/$ - see front matter
PII: S0032-3861(99)00797-1

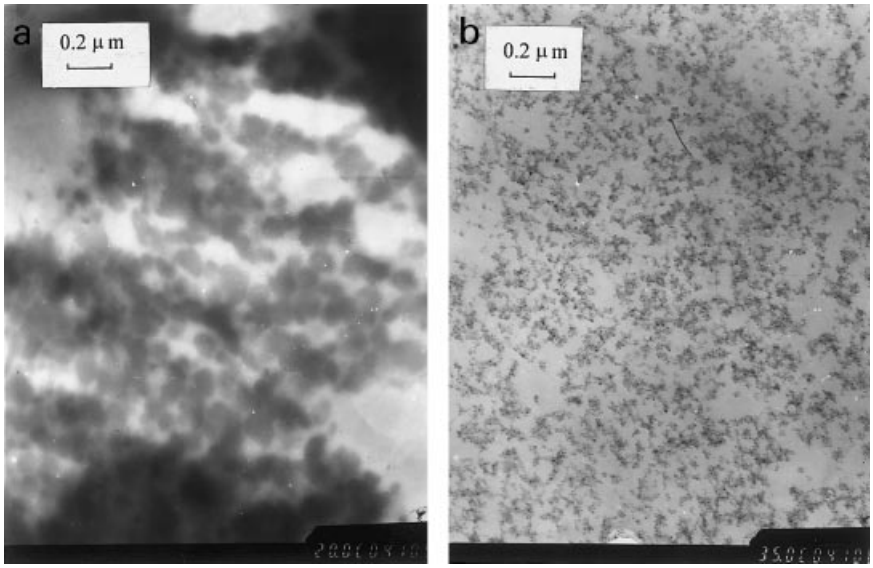

Fig. 1. TEM photomicrographs of PU/P(UBMI–BMI) IPNs: (a) semi-IPNs; and (b) full-IPNs.

First, the thermoplastic PU was synthesized in *N*,*N*-dimethylformamide (DMF) in a three-necked flask, which was equipped with reflux condenser, thermometer, heating mantle and had a constant flow of dried nitrogen. The reactive agents, which consist of 2,4-TDI, 1,4-butanediol (BD) and poly(butylene adipate) glycol (PBAG), were added stoichiometrically. The temperature was maintained at 80°C for 8 h. Then, a DMF solution of BMI and UBMI, at various weight ratios, and dicumyl peroxide (1.5 wt.% based on the weight of BMI) were added into the flask. The mixture was stirred at the same condition for 1 h, then the temperature was increased and maintained at 120°C, until the viscosity was obviously increased before gel formation, and then cooled down to room temperature. The viscous mixture was cast into a stainless-steel mold with a PTFE plate placed underneath. The solvent was removed by vacuum at 60°C in a vacuum dryer, then maintained at 120°C for 15 h, post-cured at 180°C for 1 h and demolded after cooling.

PBAG, the flexible chain incorporated into the backbone of BMI to form UBMI and used as the soft segment in PU, was synthesized by the condensation polymerization of adipic acid and BD. The average molecular weight (M_n) and acid value (I_a) were determined by traditional chemical analysis. Three kinds of PBAG were synthesized in this work: (i) $M_n = 750$, $I_a = 0.31$; (ii) $M_n = 1400$, $I_a = 0.38$; and (iii) $M_n = 2400$, $I_a = 0.15$.

2.2. Morphological studies

The morphological features and domain dimensions were examined on a Hitachi H-60 transmission electron microscope (TEM). The specimens were cut into thin strips. The cross-section of the strips was about 0.2–0.3 mm^2. They were embedded in Epon 812 epoxy resin and cured at 40°C for 60 h. The embedded specimens were first trimmed with a razor blade and then with an ultracut microtome equipped with a glass knife. An extremely smooth trapezoidal top surface was obtained with the cross-section of the polymer strip. ALKBIII microtome was used for ultra-thin microtomy. The top layer (about 1 μm) was first removed using a glass knife, then, ultra-thin sections of about 100 nm thickness were cut with a Diatome diamond knife at room temperature. The ultra-thin sections were stained by OsO_4 and mounted on 200 mesh copper grids. Finally, they were examined on TEM operating at an accelerating voltage of 80 kV.

A Hitachi S-570 scanning electron microscope (SEM) operating at an accelerating voltage of 15 kV was used to examine the fracture surface morphology. The fresh fracture surfaces of the samples were coated with gold soon after the tensile broke.

2.3. Tensile test

The tensile specimens were stretched uniaxially on KJ-500 tensile testing machine. Specimens were cut and tested at ambient temperature (25°C) at consistent cross-head speed of 100 mm min^{-1}. At least five specimens were tested for each sample.

3. Results and discussion

3.1. Morphological Studies of PU/P(BMI–UBMI) IPNs

Fig. 1 shows TEM photomicrographs of PU/P(BMI–UBMI) IPNs (full-IPNs and semi-IPNs), at a fixed weight fraction of hard segment of PU (30%), UBMI/BMI (60/40), PU/P(BMI–UBMI) (80/20), $M_{n,PBAG} = 1400$ in both PU and UBMI.

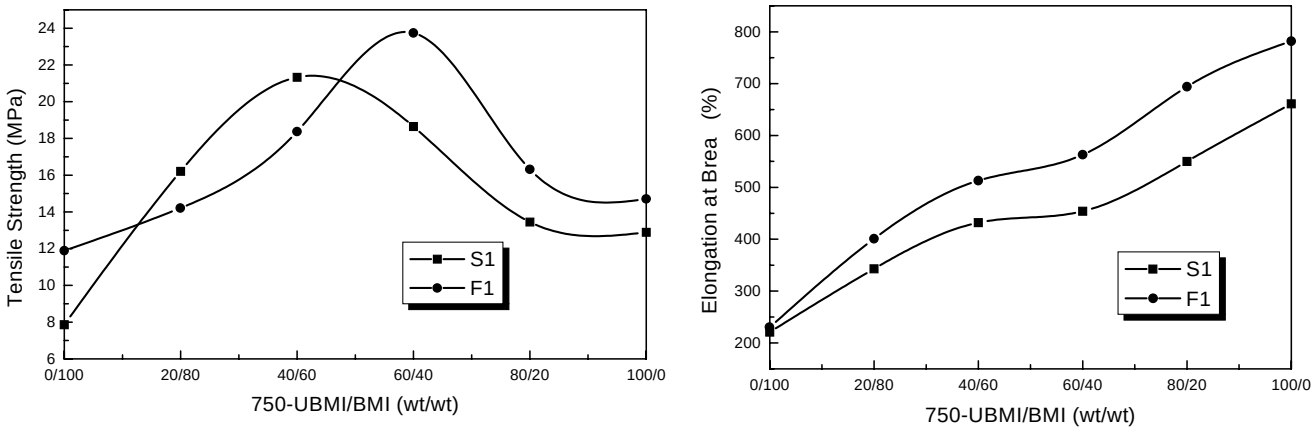

Fig. 2. Effects of UBMI/BMI on: (a) tensile strength; and (b) elongation at break of PU/P(UBMI–BMI) IPNs (M_n of PBAG in UBMI is 750; S1: semi-IPNs, F1: full-IPNs).

Generally, the morphology of PU/P(BMI–UBMI) IPNs shows a multiphase structure. The dispersed phases mainly consist of P(UBMI–BMI) and the hard segment aggregation of PU (stained by OsO_4). They are connected to each other with even and small dimension domains, whereas, the dispersed phases of neat PU are independent and have larger dimensions [7,9]. This indicates that the interpenetration concentrates on the hard segment domains. The miscibility of P(UBMI–BMI) and the hard segments of PU with this constituent, judged by the frequency shift of C–N–C in maleimide rings of FT-IR spectra [6], is obviously enhanced. This leads to the dispersing tendency of hard segment domains of PU.

The average dispersed phase dimension of semi-IPNs with this fixed constituent is 120 nm, which is far smaller than that of the hard segment aggregated domains in pure PU (1170 nm) [9]. It suggests that the large sized hard segment aggregation of PU is retarded by the enhanced hydrogen bonding and interlocking of P(UBMI–BMI), leading to a more compact packing density of the chains in domains. This conclusion can be also confirmed by DSC and FT-IR [6–8]. However, their domain dimensions are larger than that of full-IPNs, with the same constituents, except the chain extenders in PU. The average dimension of the domains in the full-IPNs is only 28 nm (Fig. 1b). Owing to covalent cross-linking in hard segment domains of PU, the mobility of large sized hard segment aggregation is retarded seriously, and this enhances the formation of large amounts of small sized hard segment domains of PU. This favors the interpenetration of the two networks to form relatively compact packing of chains. On the other hand, the flexible chains of UBMI have a tendency of dissolving into soft segment domains of PU. Both kinds of interactions force the domain dimension to get smaller. This result is similar to the traditional forced compatibility of IPNs, but their mechanisms are completely different [4,5].

PU shows phase-separated structure; the soft segment nature and its length are main factors in determining the structure. Very low molecular weight PBAG retards the hard aggregation. Only when M_n reaches about 2000, does PU show a perfect independent globular structure [9]. The dispersed phase of PU/P(UBMI–BMI) IPNs, with M_n of PBAG in PU of only 1400, shows perfect connected

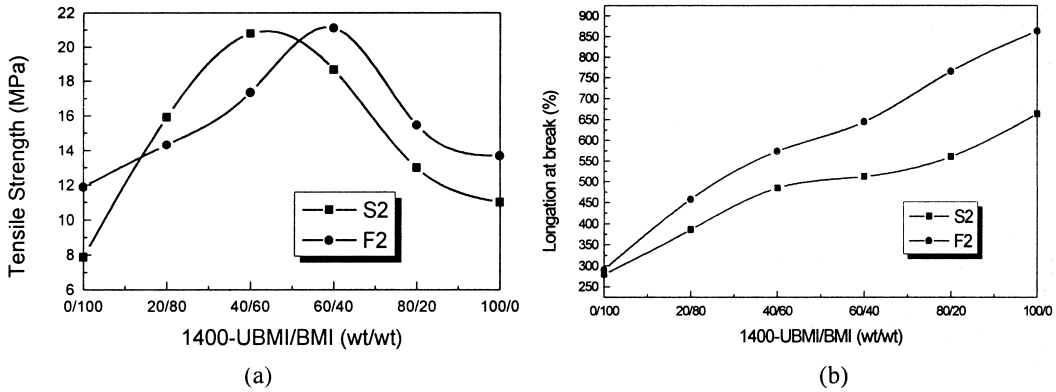

Fig. 3. Effects of UBMI/BMI on: (a) tensile strength; and (b) elongation at break of PU/P(UBMI–BMI) IPNs (M_n of PBAG in UBMI is 1400; S2: semi-IPNs, F2: full-IPNs).

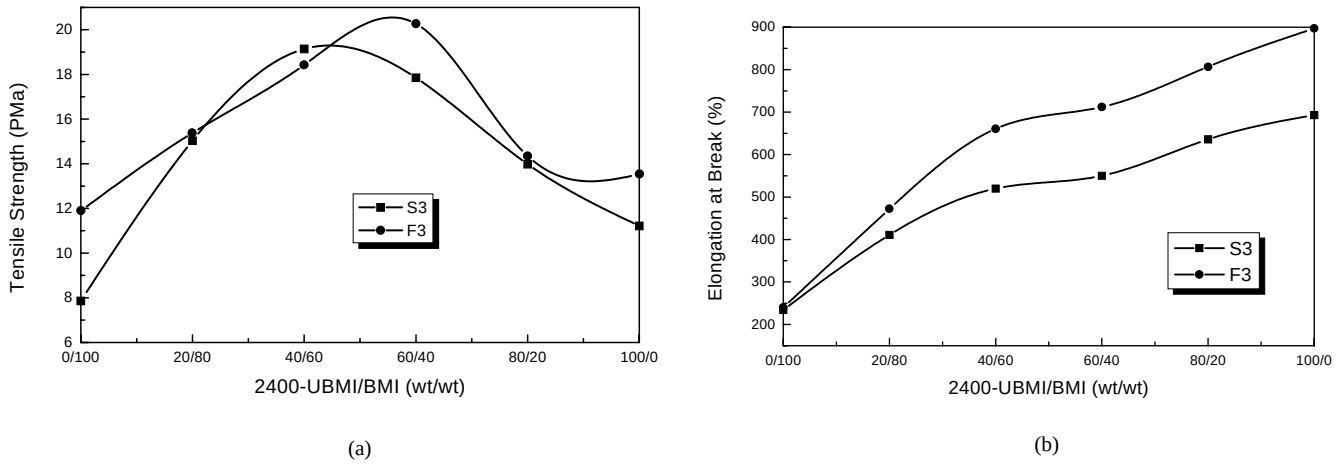

(a) (b)

Fig. 4. Effects of UBMI/BMI on: (a) tensile strength; and (b) elongation at break of PU/P(UBMI–BMI) IPNs (M_n of PBAG in UBMI is 2400; S3: semi-IPNs, F3: full-IPNs).

globular structure (Fig. 1a), which is far different from that of neat PU with the same M_n of PBAG [9]. This indicates that interpenetration of the two polymer components in hard segment domains of PU enhances phase separation of PU.

3.2. Tensile properties

3.2.1. Effect of molecular weight of PBAG in UBMI on the tensile properties

Since introduction of UBMI can enhance the miscibility of P(UBMI–BMI) and the hard segments of PU, PBAG in UBMI is the key factor affecting the miscibility. We synthesized three kinds of UBMI with various molecular weights of PBAG, to investigate the effect of molecular weight of PBAG in UBMI on the tensile properties of IPNs.

Figs. 2–4 show the tensile strength and elongation at break vs. UBMI/BMI curves for PU/P(UBMI–BMI) IPNs, with 30% hard segment in PU, $M_{n,PBAG} = 1400$ for soft segment of PU, PU/P(UBMI–BMI) = 80/20, TMP/BD = 1/3 for full-IPNs. $M_{n,PBAG}$ in UBMI are 750, 1400 and 2400, respectively, from Figs. 2–4.

Comparing the tensile properties vs. UBMI/BMI curves for semi-IPNs and full-IPNs, respectively (Figs. 2–4), we can conclude that the varying tendencies of the curves are similar for IPNs with various kinds of UBMI in P(UBMI–BMI). This indicates that these three kinds of PBAG have the same effect on the tensile properties. It may be that with PBAG in UBMI, molecular weight ranging from 750 to 2400, the enhanced interactions between P(UBMI–BMI) and the hard segments of PU are similar.

3.2.2. Effect of the ratio of UBMI and BMI on the tensile properties

From Figs. 2–4, it is interesting to observe that: (i) tensile strength increases with increasing UBMI/BMI at first, and then decreases gradually; (ii) compared with full-IPNs, the maximum value of the tensile strength appears earlier than that of full-IPNs. The maximum for semi-IPNs appears at about 40/60, while that for full-IPNs appears at about 60/40. Two questions arise when assessing the effect of each constituent of UBMI and BMI on tensile strength. First, why does the tensile strength rise steadily with the increase of UBMI, whereas, the opposite trend occurs later? Second, why does the maximum tensile strength for semi-IPNs appear at a lower ratio of UBMI and BMI than that of full-IPNs?

From microscopic observation, we can find that the morphologies of samples with different UBMI/BMI are not the same. In Fig. 5, P(UBMI–BMI) with UBMI/BMI = 20/80 for full-IPNs, aggregates to form more independent domains with larger size than that for full-IPNs with UBMI/BMI = 60/40 (Fig. 1b). The aggregations of P(UBMI–BMI) are connected with hard segment domains of PU, but far from the formation of interpenetrating structure, their domain dimensions are uneven. PBMI is

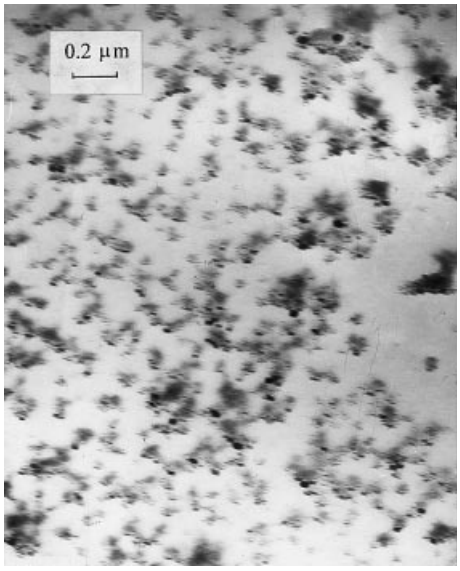

Fig. 5. TEM photomicrograph of PU/P(UBMI–BMI) full-IPNs with UBMI/BMI = 20/80 and P(UBMI/BMI)/PU = 20/80.

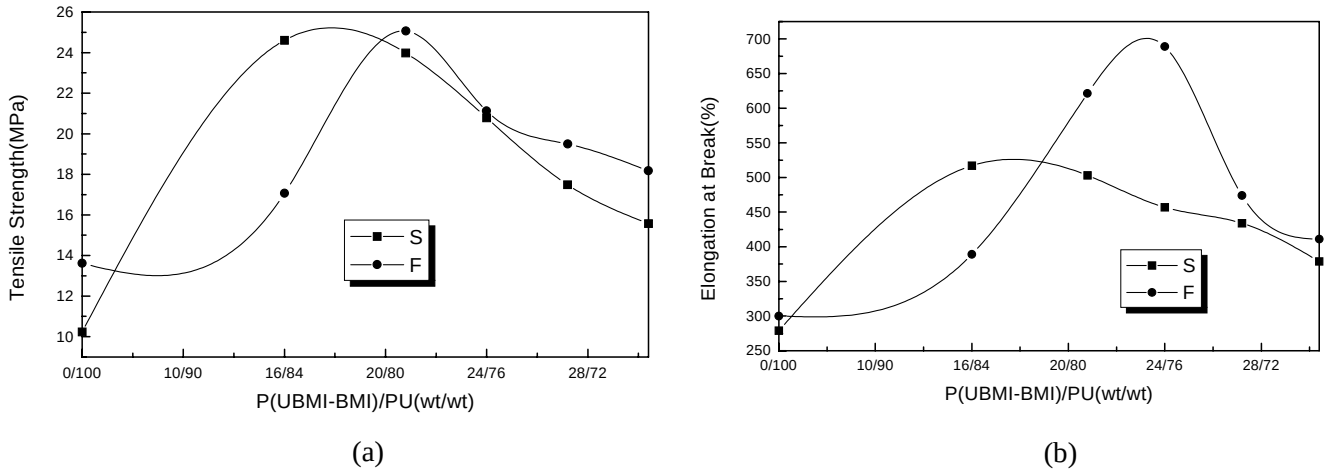

Fig. 6. Effects of P(UBMI–BMI) content on: (a) tensile strength; and (b) elongation at break of PU/P(UBMI–BMI) IPNs (M_n of PBAG in UBMI is 750; S1: semi-IPNs, F1: full-IPNs).

not compatible with PU as confirmed by investigation of the C–N–C stretching absorption peak in maleimide rings from FT-IR spectra. The effect of introducing PBMI to PU is similar to that of filling hard plastic into PU by traditional blending. Introduction of PBMI to PU has little effect on the phase separation of PU given that the content of PBMI is low [6]. When UBMI/BMI reaches 60/40, the P(UBMI–BMI) aggregation domains are surrounded by the hard segment of PU to form relatively miscible interpenetrating structure. These phenomena illustrate that incorporation of UBMI in P(UBMI–BMI) reinforces the miscibility of the two networks, leading to relatively ideal interpenetration. Interlocking of the two networks enhances the mutual entanglement of compact packing of chains and hydrogen bonding, and retards or delays pyrolysis [6]. Mechanically speaking, it increases the strength of PU/P(UBMI–BMI) IPNs. On the other hand, with the increase of UBMI, the interpenetrating structure of the dispersed phase gets more and more loose, and the hydrogen bonds of N–H are diluted largely by P(UBMI–BMI) [6]. Meanwhile, with decreasing cross-linking density, the chain packing of the interpenetrating structure gets looser, the interaction of each segment gets gradually weaker and the tensile strength also gets weaker accordingly [6–8]. This can also be confirmed by the tendency of increase of elongation at break, with the increase of UBMI/BMI. (Figs. 2b, 3b and 4b). It implies that the factors of mobility and interlocking of the chains must be considered, together, in order to satisfy the demand for comprehensive positive synergistic effect on tensile strength.

The discussion mentioned above can be extended to explain the second question. We can regard that the degree of comprehensive positive synergistic effect of the two networks' interpenetration for these two kinds of IPNs is different. Owing to cross-linking in the hard segment domains of PU for full-IPNs, while, thermoplastic of the hard segments domains of PU for semi-IPNs, the hard segments of PU for semi-IPNs are relatively movable, which needs higher cross-linking density of P(UBMI–BMI) to satisfy interlocking of the two networks to form a relatively compact interpenetrating structure of the dispersed phase. This is the reason that the ideal comprehensive positive synergistic effect of semi-IPNs and full-IPNs appears at about 40/60 and about 60/40, respectively.

In accordance with the results obtained by bimodal network studies, deformation of the bimodal is non-affine. The long chains delay the fracture of networks. Meanwhile, short chains show the effect of limited elongation on the strength and other elastic behaviors of cross-linking networks [10]. The short (long) chains deform less (more) than their counterparts in a unimodal specimen for a given amount of macroscopic deformation. Increased toughness is attributed to delays in failure of the much stiffer short chain [11,12]. Though a portion of the molecular chains reach limiting extensively early, network failure is delayed, thereby increasing the toughness [13,14]. This may be another important factor why the tensile strength appears as a peak value with the increase of UBMI in P(UBMI–BMI). (Figs. 2a, 3a and 4a).

The synergy, which causes enhanced toughness at certain mixtures in the system, may be explained as follows: reductions in the number of mechanically active chains result in an increase in the strain per network chain. In addition, increased loop formation and doubled connections occur near the same mixtures. The combination creates a reinforced network consisting of a reduced number of chains. The presence of doubled connections is more keenly felt at the mixtures in which the active chain numbers are reduced. The presence of intermediate chain lengths may increase the chances of loop formation, which is also a possible factor for the synergistic reinforcement scheme [15,16]. Such a conclusion can be confirmed by the increasing tendency of elongation at break with increase of UBMI in P(UBMI–BMI). From Figs. 2b, 3b and 4b, we can

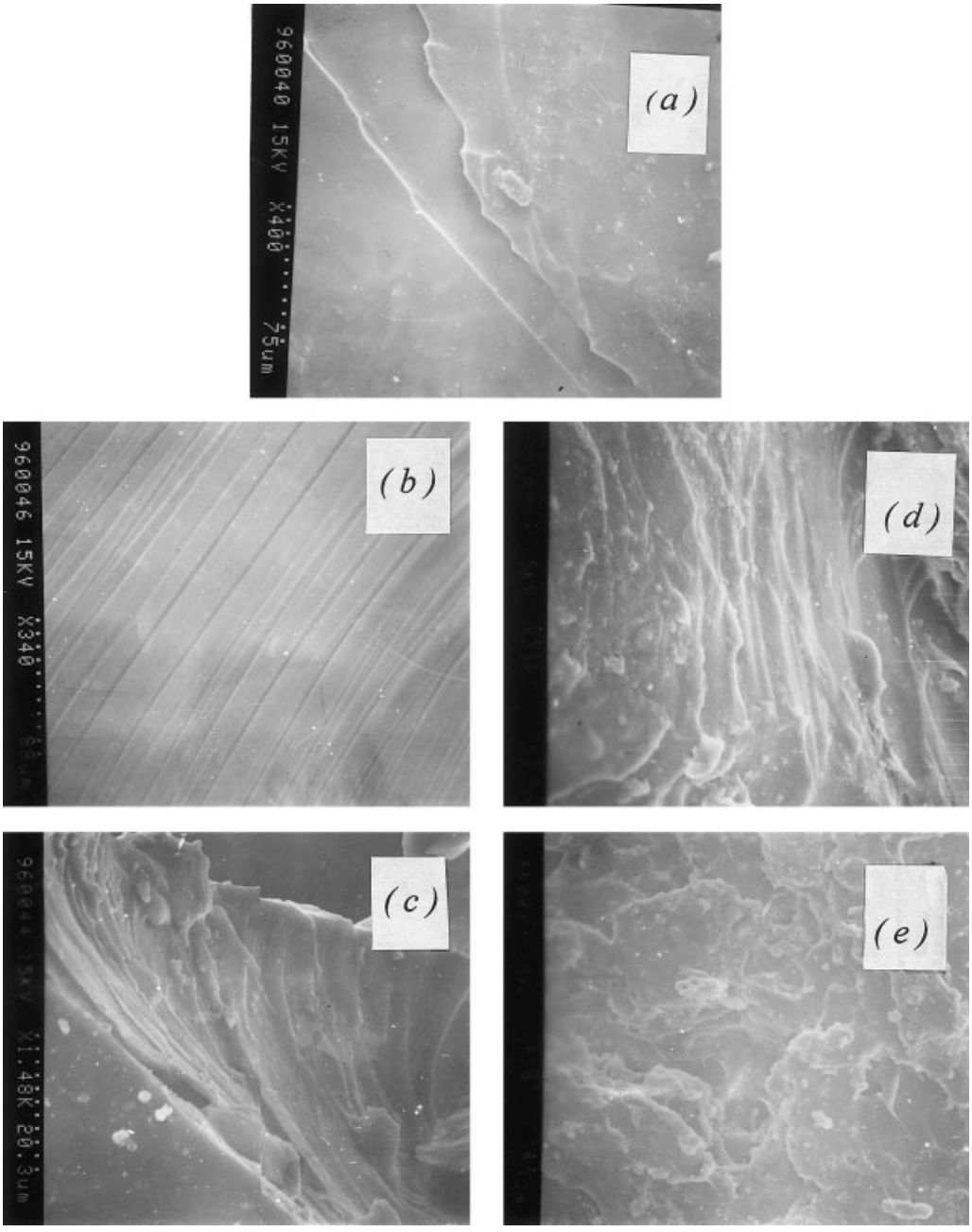

Fig. 7. SEM photomicrographs showing fracture surfaces of: (a) neat cross-linked PU; and (b)–(e) PU/P(UBMI–BMI) full-IPNs.

observe that the slopes of elongation at break vs. UBMI/BMI are lower in the range of UBMI/BMI having ideal comprehensive synergistic effect on tensile strength. We can regard that the number of mechanically active chains in this range is larger than that out of this range to form more effective interlocking loops. Efforts are underway to examine the rationality of application of results of bimodal network research to interpret the variation of toughness.

3.2.3. Effect of P(UBMI–BMI) content on the tensile properties of PU/P(UBMI–BMI) IPNs

Fig. 6 gives the tensile strength and elongation at break versus the ratio of P(UBMI–BMI) and PU curves for PU/P(UBMI–BMI) IPNs with $M_{n,PBAG} = 1400$ in PU and 750 in UBMI, 30% hard segment in PU, UBMI/BMI = 40/60 for semi-IPNs, UBMI/BMI = 60/40 and TMP/BD = 1/3 for full-IPNs.

We can observe that the maximum value of the tensile strength and elongation at break appears in the same range of P(UBMI–BMI)/PU. As to P(UBMI–BMI)/PU with the maximum value of tensile strength and elongation at break, it appears at about 12/88 for semi-IPNs, whereas, at about 18/82 for full-IPNs. The fundamental materials for the two polymer components in Figs. 2 and 6 are the same, but the

varying tendencies of the tensile properties shown in Figs. 2 and 6 are different. Fig. 2 displays the varying tendencies of the tensile properties similar to that of neat PU [9]. The explanation is the following: from Fig. 1, we can observe that the basic morphological feature of PU maintains the soft segments of PU aggregate to form the continuous phase. The phase-separated structures are more perfect than neat PU via interpenetration of P(UBMI–BMI) with the hard segments of PU.

The varying tendencies of the tensile properties shown in Fig. 6 are different from that of neat PU. After the tensile strength reaches the maximum, the elongation at break and the tensile strength both decrease with increase of P(UBMI–BMI) content. This may destroy the phase-separation structure by introducing excess of P(UBMI–BMI). This should be confirmed by TEM analysis. Further studies of this phenomenon will be published later.

3.3. Fracture surface morphological studies

Morphologies of fracture surfaces were examined using samples with $M_{n,PBAG} = 1400$, TMP/BD = 1/3 for full-IPNs.

The fracture surface of neat cross-linking PU appears to be rather brittle, a relatively smooth crack propagation area can be observed along the shear band (Fig. 7a). This suggests that the resistance of crack propagation is poor and that it can be easily broken [17]. The tensile strength and elongation at break of this material are 13.6 MPa and 300%, respectively.

For full-IPNs with P(UBMI–BMI)/PU = 20/80, UBMI/BMI = 20/80, the two networks have been poorly interpenetrated, P(UBMI–BMI) domains are connected with hard segment domains of PU to some degree (Fig. 5). The fracture surface of this material is smooth, accompanied with relatively weak shear terrace (Fig. 7b). This suggests that P(UBMI–BMI) can improve the tensile properties. But its effect is smaller than the synergistic effect of ideal IPNs. The tensile strength and elongation at break are 14.3 MPa and 458%, respectively.

For full-IPNs with P(UBMI–BMI)/PU = 20/80, UBMI/BMI = 80/20, the fractogragh shows that destroyed smoothness and ductile tearing is discernable (Fig. 7c). It suggests that this material is relatively brittle, but interpenetration retards the crack propagation to some degree [17]. The elongation at break of this sample reaches 766%. However, the hydrogen bonds have been diluted seriously, and the interpenetrating structures are loose owing to the high UBMI content in P(UBMI–BMI). The tensile strength of this sample is 15.48 MPa.

For full-IPNs with PU/P(UBMI–BMI) = 80/20, UBMI–BMI = 60/40, the morphology of fracture surface shows that extensive ductile tearing in the crack growth region is clearly discernible (Fig. 7d). This suggests that the crack propagation is greatly retarded by the incorporation of the two networks [17], the material deforms mainly via ductile tearing of the continuous phase. The dispersed IPN domains act as the acceptors of stress concentration. The tensile strength for this sample is 21.12 MPa, while the elongation at break is 689%.

For full-IPNs with PU/P(UBMI–BMI) = 84/16, UBMI/BMI = 40/60, the fractogragh reveals voiding and ductile tearing, which cannot be seen in the fractograghs mentioned above. This implies that the material is deformed by debonding in both the dispersed phase and the continuous phase. That is, fracture is caused by the debonding in the dispersed IPN domains and together with the destruction of the continuous phase of PU. The crack resource formation can be delayed and the crack propagation can be retarded greatly [17,18], leading to ideal strength with loss of toughness to some degree. The tensile strength is 25.06 MPa, and the elongation at break is 621%.

From the discussion mentioned above, the following conclusion can be obtained: because of interpenetration of the two networks, the crack resource formation can be delayed and the crack propagation can be greatly retarded. This is the essence of the comprehensive positive synergistic effect occurring in IPNs, which leads to improvement of strength and toughness.

4. Conclusion

1. The microstructure of PU/P(UBMI–BMI) IPNs was studied further using TEM. It is found that interpenetration occurs at the hard segment domains of PU, which leads to enhancement of phase separation of PU and that the dispersing tendency of the dispersed phase of IPNs causes even and small size of the dispersed phase. The dispersed phase dimensions of semi-IPNs are larger than that of full-IPNs, but far smaller than that of PU. The perfect even and small sized multiphase structure of IPNs occurs in the range of UBMI/BMI from 40/60 to 60/40.
2. Mobility and interlocking of the chains are important factors affecting the formation of perfect interpenetrating structures of the dispersed phase; they must be considered together to satisfy the demand for comprehensive positive synergistic effect on tensile properties.
3. Because of the formation of interpenetrating structure of the dispersed phases, the crack resource formation can be delayed and the crack propagation can be greatly retarded, which is the essence of the comprehensive positive synergistic effect on improvement of strength and toughness for PU/P(UBMI–BMI) IPNs.

References

[1] Hueluk V, Tomas DA, Sperling LH. Macromolecules 1972;5:340.
[2] Klemper D. J Elastoplatic 1971;3:2.
[3] Sperling LH. In: Cullbertson BM, editor. Multiphase macromolecular system, Contemporary topics in polymer science, 6. New York: Plenum, 1989. p. 665.

[4] Han QG. Chem J Chin Univ 1995;16:653.
[5] Jin SR, et al. Polym Commun 1988;29:26.
[6] Cai YL, Jiang ZM, Yang DF, Liu PS. J Appl Polym Sci 1998;68:1689.
[7] Cai YL, Jiang ZM, Liu PS. Polym Mater Sci Engng 1997;13(3):67.
[8] Cai YL, Jiang ZM, Liu PS. Polym Mater Sci Engng 1997;13(4):120.
[9] Cai YL. MD thesis. Xiangtan University, Hunan, China. 1993.
[10] Mark JE, et al. Physics properties of polymers, Washington, DC: American Chemical Society, 1984. p. 1.
[11] Monnerie L, Besbes S, Ceremelli I, Bokobza L. Macromolecules 1995;28:231.
[12] Bahar I, Erman B, Bokobza L, Monnerie L. Macromolecules 1995;28:225.
[13] Arruda EM, Boyce MC. J Mech Phys Solids 1993;41:389.
[14] Arruda EM, Przybylo PA. Polym Engng Sci 1995;35:395.
[15] Erman B, Mark JE. Macromolecules 1998;31:3099.
[16] Von Lockette PR, Arruda EM. Macromolecules 1999;32:1990.
[17] Ward IM. Mechanical properties of solid polymers, 2. New York: Wiley, 1983. p. 12 chap. 12.
[18] Hui CY, Ruina A, creton C, Kramer EJ. Macromolecules 1992;25:3848.